Magneto-impedance effect in nanocrystalline $Fe_{88}Zr_7B_4Cu$ ribbons



1997 J. Phys.: Condens. Matter 9 1951

(http://iopscience.iop.org/0953-8984/9/9/009)

J. Phys.: Condens. Matter **9** (1997) 1951–1957. Printed in the UK PII: S0953-8984(97)75881-8

# Magneto-impedance effect in nanocrystalline $Fe_{88}Zr_7B_4Cu$ ribbons

C Chen†‡, T Y Zhao‡, H Q Guo‡, L M Mei†, Y H Liu†, B G Shen‡ and J G Zhao‡

† Department of Physics, Shandong University, Jinan 250100, People's Republic of China
‡ State Key Laboratory of Magnetism, Institute of Physics, Chinese Academy of Sciences, Beijing 100080, People's Republic of China

Received 2 July 1996

**Abstract.** Magneto-impedance effects have been studied in amorphous and nanocrystalline $Fe_{88}Zr_7B_4Cu$ ribbons. Large magneto-impedance responses have been obtained in nanocrystalline samples by applying a longitudinal DC field, but not in amorphous samples. It was found that the transverse field dependences of the resistance and the reactance of nanocrystalline samples show very broad peaks at relatively high fields (above 35 Oe), while the longitudinal magnetic responses show very sharp peaks at the field of 2–7 Oe, sharing some common features with those reported for Co-based amorphous wire and ribbon samples, and can be understood from the same mechanism. It was also found experimentally that the properties of the longitudinal and transverse field dependences of the effective permeability of nanocrystalline samples correlates with those of the impedance, showing a sharp decrease for the longitudinal applied field and a slow decrease for the transverse applied field at a corresponding field value and, the higher the effective permeability, the larger is the magneto-impedance effect at a fixed frequency. $\Delta R/R_{sat} = 200\%$ and a sensitivity of 20% $Oe^{-1}$ at a low field (2 Oe) are obtained in this paper.

Recently, magneto-impedance (MI) effects have been observed in amorphous wires and ribbons [1–8], as well as in films [9], and have been attracting world-wide interest since, from a practical point of view, this phenomenon has prompted potential applications in field sensing and magnetic recording heads. The effect has been reported to be the strongest for an amorphous wire of composition $Fe_{4.3}Co_{68.2}Si_{12.5}B_{15}$ having a slight negative magnetostriction of the order of $-10^{-7}$. In the low-frequency range 1–10 kHz, which is typical of the magneto-inductive effect, the inductive component of an AC wire voltage decreases by 50% for a longitudinal field of 2–5 Oe. At higher frequencies (0.1–10 MHz) where the skin effect is essential the giant magneto-impedance (GMI) effect occurs; the amplitude of the total wire voltage decreases by 40–60% under the influence of a longitudinal field of 3–10 Oe [3].

Even though potential applications of the MI effect have already been suggested and explored, the basic mechanisms responsible for the MI effect remain not well understood. Some researchers have adopted the view of a modified skin depth, which is dominated by the effective circumferential magnetic permeability [3, 10]. Others have taken the approach of current lines distorted and dragged by magnetic domain walls oriented perpendicular to the current direction [6]. The applicability of these and other viewpoints remains to be resolved.

0953-8984/97/091951+07$19.50  

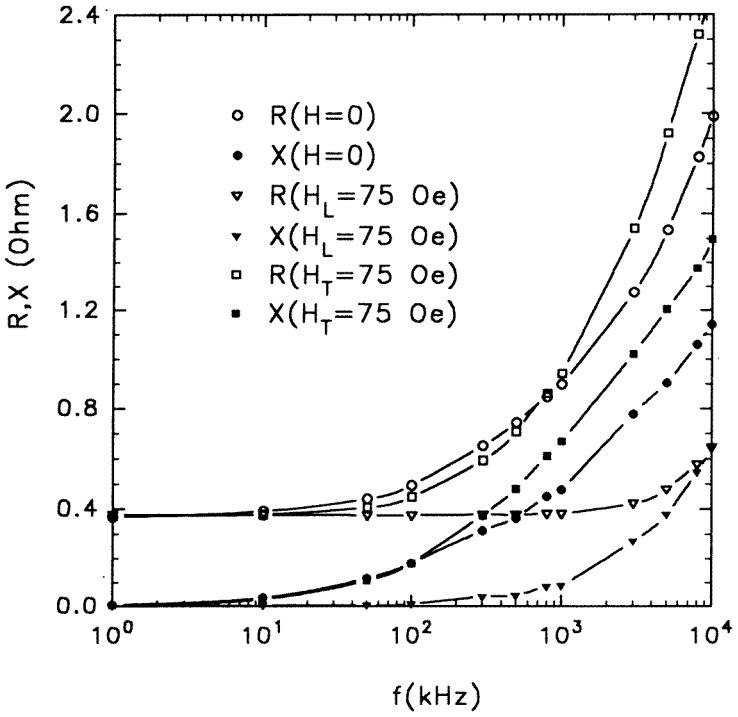


**Figure 1.** Dependences of resistance $R$ and reactance $X$ on the drive AC frequency $f$ for $Fe_{88}Zr_7B_4Cu$ ribbon sample after annealing for 1 h at 545 °C (sample SAM545), with zero applied DC field and a field of 75 Oe in the longitudinal or transverse direction.

Until now most reports on MI have been related to amorphous Co-based soft ferromagnets. It was reported recently that Fe-based nanocrystalline Fe–Cu–Nb–Si–B soft ferromagnetic ribbons and films also show a large MI effect owing to its excellent soft magnetic properties [9, 11]. In this paper, we report the MI effect in $Fe_{88}Zr_7B_4Cu$ ribbons. The longitudinal and transverse MI effects in nanocrystalline samples and their correlation with the effective permeability are studied in detail. Finally, the annealing temperature dependence of the MI effect and the effective permeability are discussed.

The as-quenched $Fe_{88}Zr_7B_4Cu$ samples with a cross section of about $0.02 \times 1.2$ mm$^2$ were prepared in an argon atmosphere by a single-roller melt-spinning method. They were first cut to 30 mm in length and then subjected to heating for 1 h at various temperatures ranging from 350 to 650 °C inside an oven that was evacuated to the order of $10^{-5}$ Torr and cooled naturally in the vacuum system. All the data presented here were obtained using an HP4192A impedance analyser. The leads of metal In were attached to the ribbons. The contact resistance was less than 1 Ω. For the effective permeability measurements, a small coil was used; one can deduce the effective permeability from the measurement of the equivalent impedance of the coil with a sample in it [12]. The samples, or the coil when $\mu'$ was measured, were connected to the analyser with four coaxial cables. The cables were 100 cm long and permitted the samples to sit within a Helmholtz coil (diameter, 30 cm), which produced a DC magnetic field $-75$ Oe $\leqslant H \leqslant 75$ Oe. The frequency responses of the current source as well as those of the sample holder and the measuring leads have been

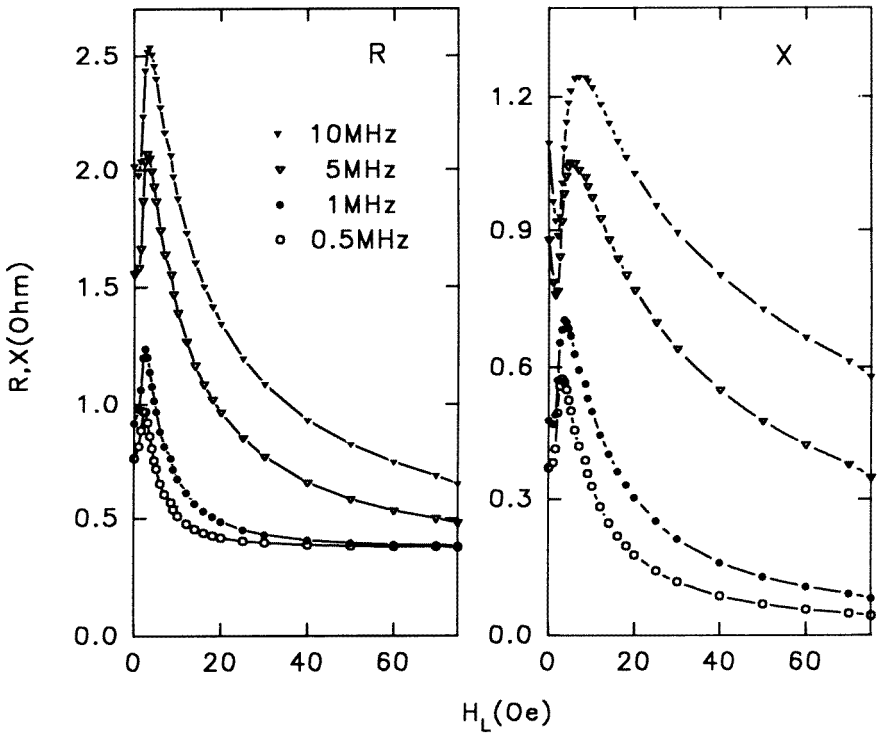


**Figure 2.** Dependences of $R$ and $X$ on the longitudinal applied field $H_L$ for sample SAM545 at the frequencies 0.5, 1, 5 and 10 MHz.

carefully checked to be free of spurious frequency effects. Both the resistive part $R(f, H)$ and the reactive part $X(f, H)$ of the complex impedance $Z(f, H) = R(f, H) + iX(f, H)$, as well as the effective permeability have been measured as functions of drive current frequency $f$ (from 1 kHz to 10 MHz) and DC magnetic field $H$ (from $-75$ to 75 Oe; only 0–75 Oe are shown in the next section). The drive current used is 10 mA. The DC field is applied in both the longitudinal and the transverse directions of the ribbons, denoted as $H_L$ and $H_T$, respectively. All the data were collected at room temperature.

X-ray diffraction has verified that the as-quenched sample and the samples annealed below 460 °C have an amorphous structure while the samples annealed at temperatures between 460 and 600 °C have a nanocrystalline structure, and the increase in annealing temperature causes the precipitation of $Fe_3Zr$, which is coincident with the results reported in [13]. Figure 1 shows the magnetoresistance $R$ and magnetoreactance $X$ spectra of the sample annealed at 545 °C for 1 h (denoted SAM545), with zero applied field and at a field (both $H_L$ and $H_T$) of 75 Oe. As the frequency increased above some critical value $f^*$, both the resistance and the reactance increased with increasing frequency. Being consistent with the skin effect, the value of $f^*$ correspond to the condition $a/\delta_m = 1$, where $a$ and $\delta_m$ represent the thickness of the sample and the skin depth, respectively [3]. At frequencies above $f^*$, the influence of the skin effect is important, and there is a large difference between the behaviours of $R$ and $X$ for $H = 0$ and for $H_L(H_T) = 75$ Oe. We note in particular that the longitudinal magnetic field of 75 Oe renders the resistance and reactance spectra nearly flat below 1 MHz for resistance but below 0.1 MHz for reactance, indicating that the

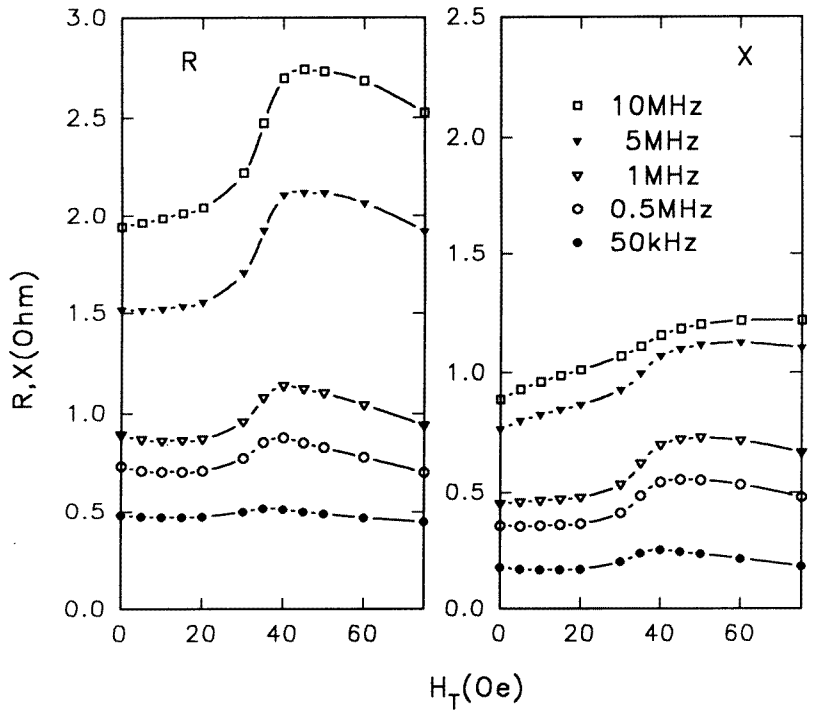


**Figure 3.** Dependences of $R$ and $X$ on the transverse applied field $H_T$ for sample SAM545 at the frequencies 50 kHz, 0.5 MHz, 1 MHz, 5 MHz and 10 MHz.

reactance is difficult to saturate. However, a transverse field of 75 Oe enhances both $R$ and $X$ at higher frequencies instead of saturating them, which means that the field of 75 Oe is far too small to saturate $R$ or $X$. The different influences of $H_L$ and $H_T$ on $R$ and $X$ will be further discussed below. We infer that both the $R$ and the $X$ spectra would tend to be flat if a large enough field is applied.

The different responses for $H_L$ and $H_T$ can be seen more clearly in figure 2 and figure 3, which show the $H_L$ and $H_T$ dependences of $R$ and $X$ for the same sample as in figure 1, namely sample SAM545, with the drive AC current frequencies being 50 kHz, 0.5 MHz, 1 MHz, 5 MHz and 10 MHz. (The curve for 50 kHz is not shown in figure 2 for clarity.) In all cases, $R$ or $X$ first increases with increasing field, then reaches a maximum value and finally decreases. Note that the peaks in figure 2 occur at lower fields while those in figure 3 occur at fields higher than 35 Oe. Another feature is that $R$ and $X$ have sharp peaks in figure 2 while they have very broad peaks in figure 3. In both cases, on the other hand, $R$ shows sharper peaks and is more easily saturated than $X$ as shown in figure 2 or figure 3. It is obvious that the curves for $H_T = 75$ Oe in figure 1 just reflect the unsaturated feature shown in figure 3. Figure 2 shares many characteristics with the results for Co-based amorphous wires reported in [1–4]; therefore, it can be understood using the same mechanism. We can deduce from this that a transverse magnetic anisotropy may exist in these ribbon samples, just as a circumferential domain structure exists in those wires. At a high enough longitudinal field, a pure rotation of the magnetic moment behaviour is expected; when the magnetization is aligned longitudinally the MI is then saturated. In

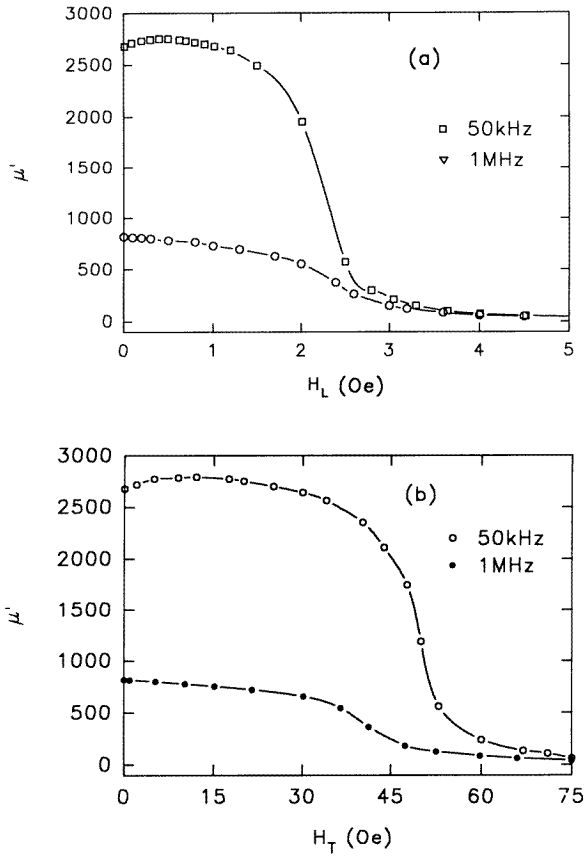


**Figure 4.** Dependences of the effective permeability $\mu'$ on (a) $H_L$ and (b) $H_T$ for sample SAM545, at the frequencies 50 kHz and 1 MHz and 1 MHz. Note that the ranges for $H_L$ and $H_T$ are different.

figure 3, $R$ and $X$ start to increase at relatively high fields, which may be caused by the demagnetization. Also, the behaviour of both $R$ and $X$ in figure 3 shows that the MI effect may be caused by the domain wall motion since $H_T$ is in the easy-axis direction.

One can obtain from figure 2 a very large effect in $\Delta R/R = (R - R_{sat})/R_{sat}$. Here we take the saturated state of the sample as the reference state for the MI ratio because this is the only well defined and history-independent state in the soft ferromagnetic material. The ratio can reach 200% at $f = 1$ MHz and would be larger at higher frequencies, but a saturation field of more than 75 Oe is needed, which is beyond our measuring condition. The impedance variation in the low-range (0–2 Oe) is very sharp, the sensitivity $[(R_{2\ Oe} - R_0)/R_0]/(2\ \text{Oe}) = 20\%\ \text{Oe}^{-1}$, where $R_{2\,Oe}$ and $R_0$ stands for the resistances at $H_L = 2$ Oe and $H_L = 0$, respectively, with $f = 1$ MHz. The reactance parts in figure 2 also show a large MI effect. However, since $X_{sat} \approx 0$ in the saturation state, the ratio $(X - X_{sat})/X_{sat}$ would be absurdly large. For the same reason described here we shall show only the annealing temperature dependence of $\Delta R/R$ at $f = 1$ MHz in figure 5 in the final part of the paper.

In order to investigate the influence of the permeability upon the MI, the effective permeability $\mu'$ versus $H_L$ and $H_T$ for the sample are studied, as shown in figure 4 for

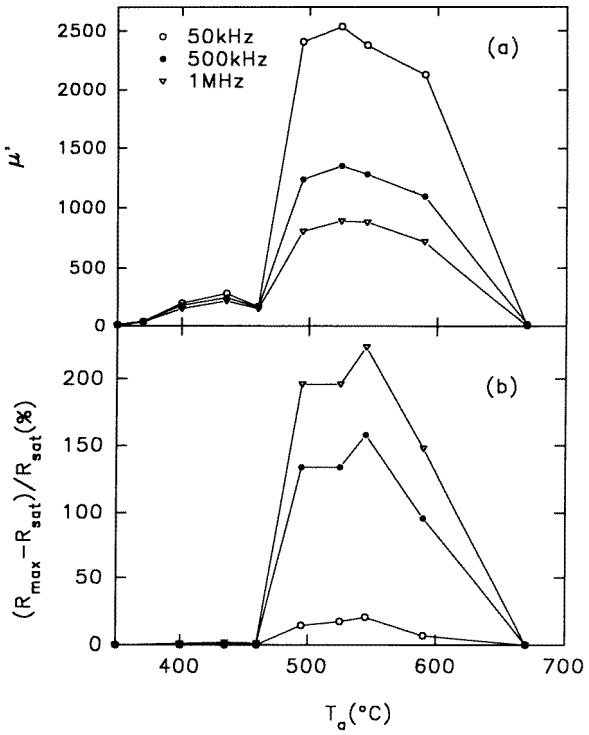


**Figure 5.** The annealing temperature dependences of (a) $\mu'$ and (b) $(R_{max} - R_{sat})/R_{sat}$ at the frequencies 50 kHz, 0.5 MHz and 1 MHz.

frequencies of 50 kHz and 1 MHz. Note that the field varies from 0 to 5 Oe for $H_L$ and from 0 to 75 Oe for $H_T$. It is observed that, with increasing $H_L$, $\mu'$ first decreases slowly, then drops dramatically at about 2.5 Oe and finally saturates. The slope at 2.5 Oe is about 3000 $Oe^{-1}$. However, $\mu'$ for $H_T$ starts to decrease slowly when $H_T$ is above 35 Oe and the maximum slope is only about 210 $Oe^{-1}$. Comparing figure 2, figure 3 and figure 4 one can find that there is a direct correlation between MI and the effective permeability $\mu'$. For high frequencies the domain wall motion is strongly damped by eddy currents. The corresponding effective permeability is greatly reduced as shown in the figure. In figure 4(a), the behaviour of $\mu'$ shows some typical properties of the transverse anisotropy and the anisotropy field is about 2.5 Oe [3]. When an AC flows through the ribbon, an easy-axis driving field will be generated. The external field $H_L$, being a hard-axis field with respect to the transverse anisotropy, suppresses the transverse magnetization by domain wall motion. As $H_L$ increases, the rotation portion of the remagnetization grows. A further increase in $H_L$ above the anisotropy field brings a rapid reduction in $\mu'$ and quickly reaches saturation as shown in figure 4(b), corresponding to the mass rotation process. On the other hand, $H_T$ is applied along the easy direction; so the magnetization process is different from above. When the field is strong enough to overcome the restraint of the eddy current, the domain wall will move until all the moment is along the transverse direction. Figure 4(b) reveals the process. Since the domain motion process is relatively slow compared with the rotation process, the slope in figure 4(b) is smaller than in figure 4(a). These responses of $\mu'$ to $H_L$ and $H_T$ result in the different MI effects through the skin depth.

Finally, we discuss the role of annealing temperature. Figures 5(a) and 5(b) show the annealing temperature dependences of the real part of the impedance ratio $(R_{max}-R_{sat})/R_{sat}$ and the effective permeability $\mu'$, respectively, where $R_{max}$ is the maximum value and $R_{sat}$ is the saturation resistance at $H_L = 75$ Oe corresponding to that in figure 2. It is obvious that large MI effects occur for samples annealed at temperatures between 500 and 600 °C, when the nanocrystalline structure is formed and the excellent soft magnetic property is produced. One can conclude that the soft magnetic property provides the basis for the GMI effect, and the skin effect causes the GMI effect to occur.

In summary, the longitudinal and transverse fields, $H = H_L$ and $H = H_T$, respectively, and frequency $f$ of the drive AC dependence of MI $Z(f, H) = R(f, H) + \mathrm{i}X(f, H)$, as well as the effective permeability of $Fe_{88}Zr_7B_4Cu$ ribbons were studied. It was found that the longitudinal field dependences of $R$ and $X$ are similar to those of the amorphous $Fe_{4.3}Co_{68.2}Si_{12.5}B_{15}$ wires but the transverse field dependence showed very broad peaks, which indicates that a similar magnetic structure may exist in the samples. The effective permeability showed corresponding properties. It was also found experimentally that only samples with a high effective permeability possess the GMI effect.

## Acknowledgments

This work was supported by the National Science Foundation of China, Doctoral Program Foundation of National Education Commission of China, and the State Key Laboratory of Magnetism, Institute of Physics, Chinese Academy of Sciences.

## References

[1] Mohri K, Kawashima K, Kohzawa T, Yoshida Y and Panina L V 1992 *IEEE Trans. Magn.* **28** 3150
[2] Mohri K, Kawashima K, Kohzawa T and Yoshida Y 1993 *IEEE Trans. Magn.* **29** 1245
[3] Panina L V, Mohri K, Kushida K and Noda M 1994 *J. Appl. Phys.* **76** 6198
[4] Beach R S and Berkowitz A E 1994 *Appl. Phys. Lett.* **64** 3652
[5] Mandal K and Ghatak S K 1983 *Phys. Rev.* B **47** 14 233
[6] Machado F L A, da Silva B L, Rezende S M and Martins C S 1994 *J. Appl. Phys.* **75** 6563
[7] Velázquez M, Vázquez M, Chen D X and Hernando A 1994 *Phys. Rev.* B **50** 16 737
[8] Rao K V, Humphrey F B and Costa-Krämer J L 1994 *J. Appl. Phys.* **76** 6204
[9] Sommer R L and Chien C L 1995 *Appl. Phys. Lett.* **67** 3346
[10] Beach R S and Berkowitz A E 1994 *J. Appl. Phys.* **76** 6029
[11] Chen C, Luan K Z, Liu Y H, Mei L M, Guo H Q, Shen B G and Zhao J G 1996 *Phys. Rev.* B **54** 6092
[12] Standard method of test for alternating current magnetic properties of materials using the modified Hay bridge method with 25 cm Epstein frame 1996 *ASTM Stand.* A347-68
[13] Suzuki K, Kataoka N, Inoue A, Makino A and Masumoto T 1990 *Mater. Trans. Japan Inst. Met.* **32** 743